Polskie Towarzystwo Materiałów Kompozytowych
Polish Society of Composite Materials

25: 2 (2025) 75–81

COMPOSITES THEORY AND PRACTICE

ISSN (online): 2299-128X

Michał Żakowski*, Grzegorz Cieślak, Dariusz Oleszak

Faculty of Materials Science and Engineering, Warsaw University of Technology, 141 Wołoska St., 02-507 Warsaw, Poland
* *Correspondence:* michal.zakowski2.stud@pw.edu.pl

Received (Otrzymano) 28.01.2025

HIGH-ENTROPY AlCoCuFeNi MATRIX COMPOSITES REINFORCED WITH TUNGSTEN CARBIDE

https://doi.org/10.62753/ctp.2025.06.2.2

In the present study, metallic-ceramic composites were fabricated, with an equimolar high-entropy AlCoCuFeNi alloy as the matrix, and tungsten carbide WC (5 and 10% by volume) as the reinforcing phase. Induction melting and arc melting techniques were used for composite preparation. The metallic matrix of the composite exhibited a two-phase structure consisting of FCC and BCC solid solutions. Microscopic investigations revealed a dendritic microstructure of the matrix, in which the WC particles were distributed non-homogeneously, regardless of the melting method. Strong precipitation of the chemical composition in the matrix was observed, with interdendritic regions enriched in copper and dendrites enriched in aluminium, nickel and iron. Additionally, besides WC particles, two types of precipitates, with various morphology, were observed in the matrix. The addition of tungsten carbide particles resulted in an increase in the composite hardness from approximately 273 HV for the high-entropy alloy to as high as 332 HV for the composite. The appearance of the precipitates can be attributed to the chemical reaction between the liquid matrix and WC, resulting in the formation of complex carbides.

Keywords: **high-entropy alloys, metal-ceramic composites, induction melting, arc melting, microstructure, hardness**

INTRODUCTION

The term high-entropy alloys (HEAs) were first proposed two decades ago by Yeh and his research team. They defined these materials as containing at least five metallic elements, with an equal or nearly equal proportion of each (not less than 5% and not more than 35%) [1]. Over the years, the definition of high-entropy alloys has been modified several times, particularly regarding the number of elements in the alloy. Initially, HEAs usually consisted of four or five alloying elements (with an equimolar composition), but this number has gradually increased over time [2]. In addition, the concept of configurational entropy, which plays a key role in distinguishing high-entropy alloys from other metallic systems, has also evolved. A new category of multi-component alloys emerged – in addition to high entropy alloys, also alloys with medium configurational entropy [3]. Since 2004, the year in which the first article related to HEAs was published, a huge increase in the number of publications devoted to this group of materials has been observed [4]. These developments reflect ongoing efforts to better characterise the thermodynamic stability and phase formation behaviour of HEAs, which are affected by their increased compositional complexity.

HEAs are distinguished from traditional alloys by four effects that are exclusive to them [5]. These effects can be categorised as the high-entropy effect, lattice distortion effect, slow diffusion effect and the “cocktail” effect.

HEAs are not mere scientific curiosities; they have begun to find application across a spectrum of industries. In the medical field, they are used as

implant coatings. They will be available as a material for use in energy, particularly as fusion and nuclear reactor materials [6, 7]. Additionally, they have been utilized in the electrical industry owing to their low-melting characteristics as solders [8]. They also serve as potential substitutes for superalloys, like Inconel and Haynes alloys [9, 10].

The investigation of implant materials is focused on alloys containing titanium, zirconium, tantalum and hafnium, among others. These elements can be found in medium and high-entropy alloys, including TiZrHf (111 GPa), TiZrNbHfTa (103 GPa), TiZrNbHf (83 GPa), and TiZrTaHf (86 GPa). These materials have a lower Young's modulus than commercially used Ti6Al4V alloys (116 GPa) [11]. A reduction in the Young's modulus value of a metallic implant results in a closer matching to that of natural bone, thus reducing the probability of stress shielding at the implant-bone interface.

It is also possible that HEAs could become a crucial component in the construction of nuclear power plants, particularly those based on nuclear fusion. The action of radiation on the reactor material can result in the formation of defects, which are also known as “helium bubbles”. The lattice distortion of HEAs enables this phenomenon to be reduced, thereby extending the operational lifetime of the reactor. A comparison of the microstructure of the WMoTaVNb alloy exposed to helium plasma (simulating reactor operation) with that of tungsten reveals a significantly lower number of helium bubbles with smaller dimensions in the HEA [6].

Moreover, some studies have indicated that a specific group of HEAs exhibits excellent mechanical properties at elevated temperatures, even better than Inconel 718 and Haynes 230 superalloys. These HEAs are based on Nb, Mo, Ta, W and Hf (for example, the equimolar alloy VNbMoTaW). It is possible, that over time, these alloys may replace the previously mentioned superalloys in applications such as jet engines or gas turbine blades resulting from their ability to maintain high strength values at elevated temperatures [10].

One of the trends observed in the field of metal-ceramic composites is the use of high-entropy alloys for the matrix of composites. This idea was born out of the desire to increase the hardness, reduce tribological wear [12] or improve other strength properties of composites in comparison to those previously utilising metals and alloys as their matrix [13]. A further motivation for creating this type of material is the desire to exploit the distinctive characteristics that high-entropy alloys can offer. They include enhanced corrosion resistance, resistance to oxidation at high temperatures and the absence of magnetic properties, which can present a challenge in certain applications [14].

Without any doubt, the use of high-entropy alloys in the development of metal-ceramic composites could provide many surprising discoveries and translate into wider practical applications of these advanced composites.

The aim of this study is to fabricate a metal-ceramic composite in which the matrix is a high-entropy AlCoCuFeNi alloy, and the ceramic phase is tungsten carbide, as well as to investigate the microstructure and selected properties of the resulting composite.

MATERIALS, SAMPLE PREPARATION METHODS AND EXPERIMENTAL DETAILS

An equimolar AlCoCuFeNi high-entropy alloy was selected as the matrix for the metal-ceramic composite reinforced with WC particles. The alloy is characterised by a two-phase structure, composed of a mixture of BCC and FCC phases with a dendritic microstructure. The two-phase structure of the alloy is a consequence of the high content of Al, which serves to stabilise the BCC phase, and the high content of Cu, which stabilises the FCC phase [15].

For fabrication of the composites pure metals were used (purity at least 99.9%) for the metallic matrix and WC powder particles (average particle size 80 μm, measured by means of a Kamika Instruments Mini 3D particle size analyser) as the reinforcement. The contribution of the ceramic phase was 5 and 10 % by volume. The metallic AlCoCuFeNi alloy was prepared in advance by arc melting and induction melting. In both methods of composite preparation, the WC powders were cold pressed. During the composite fabrication process by arc melting, the piece of metallic alloy and powder compact were placed together in an arc

furnace block and melted several times under argon protective atmosphere. In the induction melting process, the ceramic WC compact was placed at the bottom of the quartz tube and the HEA on top of it. After melting of the metallic component, the liquid alloy infiltrated the ceramic compact. The melting process, performed under argon atmosphere, was repeated three times to ensure better homogeneity of the composites.

The following material designation system was employed to identify the samples: XXWC_Y. In this system, XX denotes the volume content of tungsten carbide in the sample, representing a percentage value. Y denotes the melting method of the metallic phase, with the following values: "I" denotes induction melting and "A" denotes arc melting.

Diffraction analysis was conducted using a Rigaku MiniFlex II X-ray diffractometer, equipped with Cu Kα radiation (λ = 1.5418 Å). All the measurements were conducted with the following parameters: step 0.05°, counting time 3 s, and 2θ range from 20° to 120°. The microstructure of the composites was studied by means of a Keyence VHX-7000 digital light microscope. The samples for observations were subjected to a standard procedure of polishing and etching. The following etching reagent was applied: 68 cm^3 of water, 16 cm^3 of nitric acid and 16 cm^3 of hydrofluoric acid. For all the evaluated materials, SEM observations in topographic contrast mode SE were performed utilising a Hitachi S3500 scanning electron microscope. In addition, elemental distribution mapping was also performed for all the samples by the EDS technique. To analyse the hardness of the studied materials, the Vickers method was employed with a constant loading of 10 kG (98.07 N). Three indentations were made in each material and then the result was averaged.

RESULTS

Microscopic observations of the 0WC_I and 0WC_A samples show a typical dendritic microstructure consisting of light dendrites DR and a dark interdendritic component ID (Fig. 1). Arc melting resulted in a smaller grain size of the alloy than induction melting.

The microstructures of composite samples 5WC_I and 5WC_A reveal both polyhedral ceramic particles (blue arrows in Fig. 1), as well as a new acicular phase (marked by a yellow circle inFig. 1), which is not observed in the microstructure of the AlCoCuFeNi alloy. In addition, for the arc-melted composite (red circle in Fig. 1 of 5WC_A), the presence of small precipitates with an "arrow-like" morphology, often radiating from a single point and quite uniformly distributed in the HEA matrix was observed.

The 10WC composite samples, both after induction melting (10WC_I) and after arc melting (10WC_A), show strong agglomeration in the lower part of the composites – particularly evident in sample 10WC_I (Fig. 1). The carbide particles must have sedimented intensively when the metallic matrix was in liquid form. This phenomenon can be related to the significant difference in the density of metallic matrix and WC, 7.47 gcm^{-3} and 15.63 gcm^{-3}, respectively. The experiments suggest that the 10 vol.% WC reinforcement in the AlCoCuFeNi alloy matrix is too high to achieve a homogeneous microstructure throughout the composite.

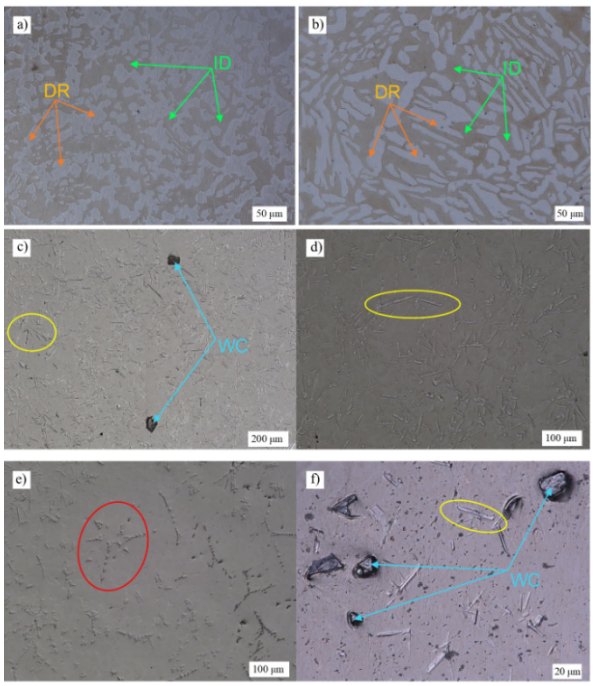

Fig. 1

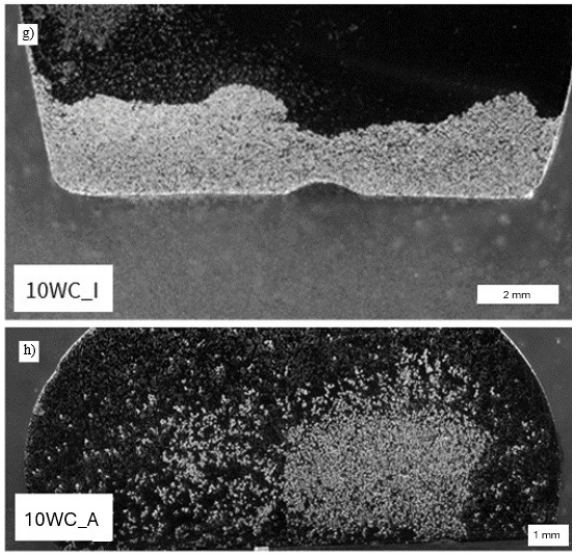

Fig. 1. Microstructures of investigated materials (a-h) depending on ceramic phase content and on preparation method (digital light microscope)

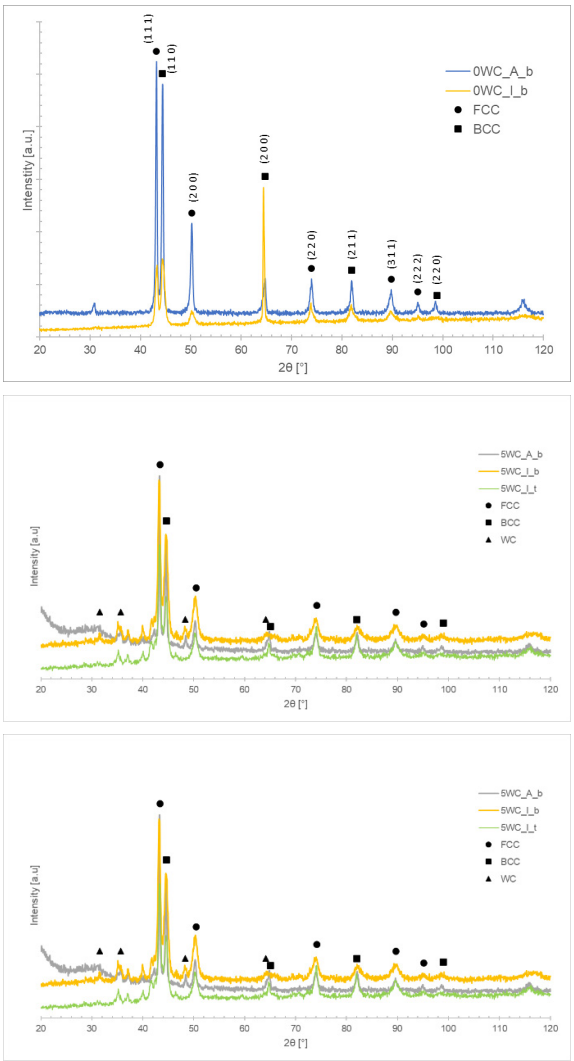

Fig. 2. Diffractogram sequence for: a) pure AlCoCuFeNi, b) composites containing 5 vol.% WC, c) composites containing 10 vol.% WC melting via both methods ("_b" – bottom edge of sample, "_t" – top edge of sample).

X-ray studies of the bottom surfaces of reference samples 0WC_I and 0WC_A (Fig. 2a) showed the existence of two solid solutions: FCC and BCC. The diffraction lines of the solid solutions and WC were observed in all the XRD patterns for the 5WC composites (Fig. 2b). Their intensities are slightly higher for the pattern taken on the bottom surface of the samples. The diffraction data set for the composites with 10 vol.% WC (Fig. 2c) revealed strong peaks derived from WC for sample 10WC_I_b, which are practically not observed in the upper surface of this sample owing to the non-uniform distribution of the ceramic in the composite volume. The unidentified peaks observed in the diffraction patterns may originate from the unidentified acicular or arrowlike precipitates present in these composites.

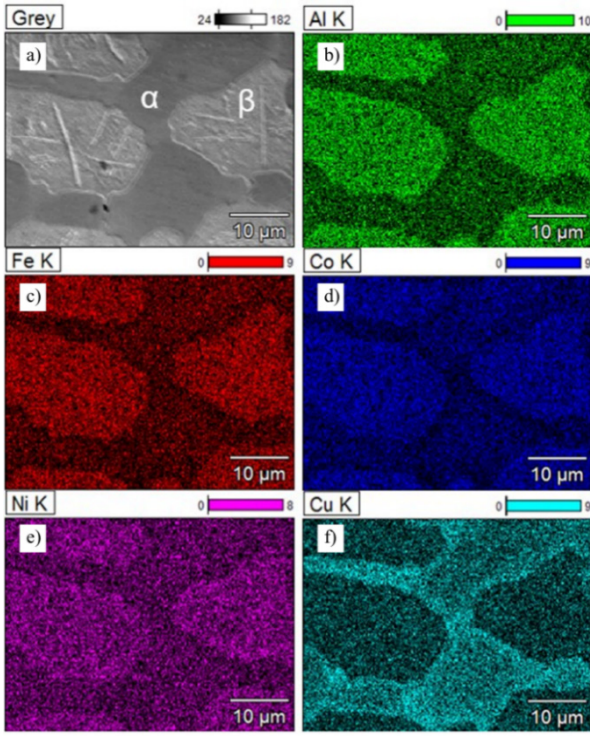

Fig. 3. Element mapping (a-f) of AlCoCuFeNi alloy matrix (made on 10WC_I composite)

EDS analysis mapping showed that the two phases of the high-entropy matrix have different chemical compositions. This is best illustrated by the analysis carried out on the 10WC_I sample at a location away from the carbides: the darker phase is rich in Cu, while the lighter phase is rich in aluminium, iron and nickel. Cobalt is fairly evenly distributed in both phases (Fig. 3). The ap-

parent chemical precipitation is seen in all the microstructures and confirms previous findings for this alloy. It can be concluded that the darker phase is the α-solid solution FCC and the lighter β-solid solution BCC [16].

EDS analysis of the acicular precipitates (Fig. 4 – 5WC_I b) present in all the types of composites and the arrowlike precipitates (Fig. 4 – 5WC_A) in the arc-melted composites indicates that the tungsten carbide is likely to react with the HEA elements. The multi-walled WC particles contain a 1:1 atomic ratio of C to W atoms (Table 1 – 10WC_I and 5WC_I). The arrow-shaped precipitates contain an increased Cu content and a similar content of the other elements except aluminium (Table 1 – grey-blue frame). The acicular precipitates, on the other hand, have almost twice the amount of Co and Fe, but a lower amount of copper than the arrowlike precipitates (Table 1 – red frame). The proportion of Ni is similar in both precipitates. The increased proportion of Fe and Co in these phases may explain why a depletion of the α-phase in these elements is observed.

The ceramic tungsten carbide should not react with the metallic matrix melted by induction/arc melting. It is suggested that during arc melting, the melting temperature of the carbide was locally exceeded (2870°C), resulting in the formation of a complex carbide containing Fe and Co in addition to W, with an arrowlike morphology. Importantly, significant diffusion of C into the metallic matrix was also observed (Table 1 – green frame).

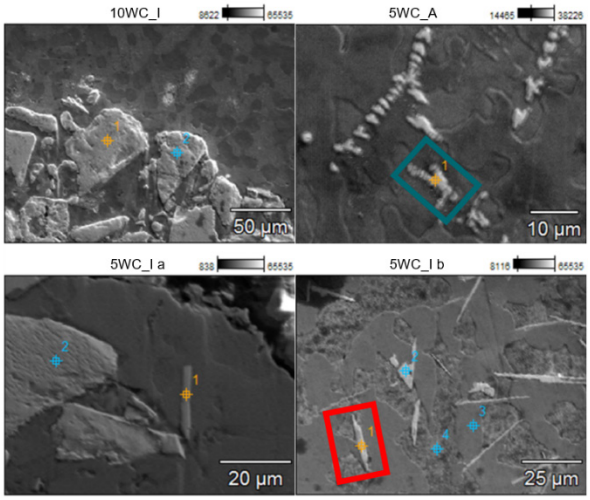

Fig. 4. EDS analysis points of microstructural elements of selected composites

Table1. **Measured values of atomic content of elements, together with measurement uncertainties, determined from selected locations in Fig. 4**

Sampling point	C [%]	W [%]	Al [%]	Co [%]	Cu [%]	Fe [%]	Ni [%]	S [%]	Au [%]
10WC_I: point 1	27.08 +/- 7.40	72.86 +/- 0.72	-	-	-	-	-	-	0.05 +/-0.05
10WC_I: point 2	58.83 +/- 6.51	40.24 +/- 0.40	-	0.20 +/- 0.11	-	0.56 +/- 0.10	-	0.12 +/-0.09	0.05 +/-0.05
5WC_A: point 1	48.36 +/- 1.58	23.39 +/- 0.28	-	6.35 +/- 0.15	10.08 +/- 0.21	5.70 +/- 0.13	6.12 +/- 0.16	-	-
5WC_I a: point 1	32.95 +/- 1.59	34.65 +/- 0.38	-	12.99 +/- 0.22	0.94 +/- 0.17	13.31 +/- 0.20	5.00 +/- 0.19	0.17 +/- 0.09	-
5WC_I a: point 2	55.56 +/- 1.78	43.54 +/- 0.41	-	-	0.25 +/- 0.16	0.63 +/- 0.11	-	0.03 +/- 0.10	-
5WC_I b: point 1	28.36 +/- 1.41	34.64 +/- 0.37	2.22 +/- 0.09	10.57 +/- 0.20	6.17 +/- 0.21	11.29 +/- 0.18	6.77 +/- 0.19	-	-
5WC_I b: point 2	29.40 +/- 1.41	36.63 +/- 0.38	2.30 +/- 0.09	13.01 +/- 0.22	1.23 +/- 0.17	12.68 +/- 0.20	4.76 +/- 0.18	-	-
5WC_I b: point 3	16.64 +/- 1.04	0.33 +/- 0.11	9.96 +/- 0.12	18.67 +/- 0.20	23.14 +/- 0.27	12.53 +/- 0.15	18.73 +/- 0.23	-	-
5WC_I b: point 4	25.54 +/- 0.92	-	11.20 +/- 0.11	15.33 +/- 0.17	17.55 +/- 0.21	12.89 +/- 0.14	17.50 +/- 0.20	-	-

Arrowlike precipitation

Acicular precipitation

Table 2. **Results of hardness measurements**

Sample	Hardness [HV_{10}]
0WC_I	273 ± 20
0WC_A	276 ± 7
5WC_I	328 ± 13
5WC_A	309 ± 12
10WC_I	323 ± 32
10WC_A	332 ± 23

It can be observed that the melting method of the HEA has practically no effect on the change in hardness of all the investigated materials (Table 2). The addition of WC increases the hardness of the composites compared to the pure HEA. However, its 10% content is not observed to significantly raise the hardness of the composites compared to its equivalent with the 5% WC content. This probably results from the non-homogeneous distribution of the ceramic phase in the volume of the material.

DISCUSSION AND CONCLUSIONS

In the present study, an attempt was made to produce a metal-ceramic composite with a high-entropy alloy as the matrix. Based on literature data, the AlCoCuFeNi alloy matrix was selected. This matrix, which exhibits a two-phase structure of FCC and BCC solid solutions, is an example of a material that deviates from the theoretical assumptions of phase structure based on the VEC criterion proposed by Guo [17] and other researchers [16, 18]. By adding tungsten carbide, commonly used in metal-ceramic composites, to the

selected matrix, the aim was to investigate how the addition of 5 and 10 vol.% WC would affect the microstructure, phase structure and hardness of the AlCoCuFeNi-WC composite.

To produce the composite samples, an original method was proposed to introduce the ceramic particles into the liquid melt using two melting methods: induction and arc melting. In both cases, the produced composite samples had to be remelted several times due to problems with the introduction and distribution of the ceramics in the liquid metal matrix. These problems were a consequence of the significant difference in density between the metallic alloy (7.47 gcm-3) and tungsten carbide (15.63 gcm-3). Despite several remelts, it was not possible to obtain a homogeneous distribution of the ceramics in the volume of all the composite samples.

For the pure AlCoCuFeNi alloy – without the addition of ceramics – two solid solutions of FCC and BCC with similar proportions were detected. This observation was made for both the manufacturing methods. The structure of the pure high-entropy alloy shows a dendritic character with pronounced chemical precipitation – the dendrites are significantly enriched in aluminium, nickel and iron, while the interdendritic regions are highly enriched in copper. The observed precipitation is confirmed by literature data [16].

The studies of the HEA-WC composites confirmed the difficulties associated with the homogeneous distribution of the ceramics in the metallic matrix – although the carbide was relatively uniformly distributed in the volume of the composite samples with 5 vol.% ceramics, it was observed that it tended to be located close to the edges of the samples. This was observed for both the manufacturing methods. In the composites with the higher ceramic content, the WC was completely sedimented in the liquid metal. As a result, strong agglomeration of the carbide particles in the lower part of the sample was observed in the cross-section of the composites with the 10% WC content.

The addition of ceramic reinforcement to the matrix did not affect the phase structure of the solid solutions. Nevertheless, it is important to note that new phases were observed in the microstructure of the HEA-WC composites: acicular and ones resembling small arrows radiating outwards. The acicular precipitates were observed in both the induction and arc melting methods, while the arrowlike ones were present in the composites after arc melting only. Analysis of the chemical composition showed that the acicular phase contains iron and cobalt in addition to W and C atoms, while the second type of precipitates contain a significant amount of copper in addition to the previously mentioned elements.

The identification of the new phases, as well as the investigation of the mechanism of their formation, are beyond the scope of this work, however, it can only be suggested that the formed precipitates are the result of the reaction of the tungsten carbide with the liquid metal of the matrix.

The hardness of the composites obtained by the two methods does not differ significantly. It is not possible either to see that the increase in the proportion of ceramic from 5 to 10 % by volume has any significant effect on the rise in the hardness of the composites. For instance, the hardness of the 5WC_I material is 328±13 HV, while for the 10WC_I material it is 323±32 HV. This may be because it was not possible to achieve completely uniform distribution of the ceramics in the matrix of the composites due to differences in the density of the ceramics in relation to the matrix.

In this study an original method for manufacturing metallic-ceramic composites was applied to successfully obtain AlCoCuFeNi-WC composites. Nonetheless, owing to significant differences in the density of the metallic matrix and ceramic phase, the distribution of the WC particles in the HEA matrix was not homogeneous. Additionally, a chemical reaction between WC and the metallic elements from the matrix was observed, resulting in the formation of new phase(s) in the form of precipitates.

Acknowledgements

The financial support from the subsidy of the Faculty of Materials Science and Engineering, WUT, is greatly appreciated.

REFERENCES

[1] Yeh J.-W., Chen S.-K., Lin S.-J., Gan J.-Y., Chin T.-S., Shun T.-T., et al. Nanostructured High-Entropy Alloys with Multiple Principal Elements: Novel Alloy Design Concepts and Outcomes. Adv Eng Mater 2004;6:299–303. https://doi.org/10.1002/adem.200300567.

[2] Gao M.C., Yeh J.-W., Liaw P.K., Zhang Y., editors. High-Entropy Alloys. Cham: Springer International Publishing; 2016. https://doi.org/10.1007/978-3-319-27013-5.

[3] Miracle D., Miller J., Senkov O., Woodward C., Uchic M., Tiley J. Exploration and Development of High Entropy Alloys for Structural Applications. Entropy 2014;16:494–525. https://doi.org/10.3390/e16010494.

[4] Li W., Xie D., Li D., Zhang Y., Gao Y., Liaw P. K. Mechanical behavior of high-entropy alloys. Prog Mater Sci 2021;118:100777. https://doi.org/10.1016/j.pmatsci.2021.100777.

[5] Yeh J.-W. Recent progress in high-entropy alloys. Ann Chim Sci Matér 2006;31:633–48. https://doi.org/10.3166/acsm.31.633-648.

[6] Wang K., Yan Y., Xiong Y., Zhao S., Chen D., Woller K. B. Enhanced radiation resistance of W-based HEA under helium-ion irradiation conditions. J Nucl Mater 2024;588:154761. https://doi.org/10.1016/j.jnucmat.2023.154761.

[7] Mackova A., Havránek V., Mikšová R., Fernandes S., Matejicek J., Hadraba H., et al. Radiation damage evolution in High Entropy Alloys (HEAs) caused by 3–5 MeV Au and 5 MeV Cu ions in a broad range of dpa in connection to mechanical properties and internal morphology. Nucl Mater Energy 2023;37:101510. https://doi.org/10.1016/j.nme.2023.101510.

[8] Liu Y., Pu L., Yang Y., He Q., Zhou Z., Tan C., et al. A high-entropy alloy as very low melting point solder for advanced electronic packaging. Mater Today Adv 2020;7:100101. https://doi.org/10.1016/j.mtadv.2020.100101.

[9] Senkov O.N., Wilks G.B., Scott J.M., Miracle D.B. Mechanical properties of Nb25Mo25Ta25W25 and V20Nb20Mo20Ta20W20 refractory high entropy alloys. Intermetallics 2011;19:698–706. https://doi.org/10.1016/j.intermet.2011.01.004.

[10] Ye Y.F., Wang Q., Lu J., Liu C.T., Yang Y. High-entropy alloy: challenges and prospects. Mater Today 2016;19:349–62. https://doi.org/10.1016/j.mattod.2015.11.026.

[11] Feng J., Tang Y., Liu J., Zhang P., Liu C., Wang L. Bio-high entropy alloys: Progress, challenges, and opportunities. Front Bioeng Biotechnol 2022;10:977282. https://doi.org/10.3389/fbioe.2022.977282.

[12] Li Z., Fu P., Hong C., Chang F., Dai P. Tribological behavior of Ti(C, N)-TiB2 composite cermets using FeCoCrNiAl high entropy alloys as binder over a wide range of temperatures. Mater Today Commun 2021;26:102095. https://doi.org/10.1016/j.mtcomm.2021.102095.

[13] Yadav S., Zhang Q., Behera A., Haridas R. S., Agrawal P., Gong J., et al. Role of binder phase on the microstructure and mechanical properties of a mechanically alloyed and spark plasma sintered WC-FCC HEA composites. J Alloys Compd 2021;877:160265. https://doi.org/10.1016/j.jallcom.2021.160265.

[14] Liu B., Wang J., Chen J., Fang Q., Liu Y. Ultra-High Strength TiC/Refractory High-Entropy-Alloy Composite Prepared by Powder Metallurgy. JOM 2017;69:651–6. https://doi.org/10.1007/s11837-017-2267-0.

[15] Matusiak K., Berent K., Marciszko M., Cieslak J. The experimental and theoretical study on influence of Al and Cu contents on phase abundance changes in Al Cu FeCrNiCo HEA system. J Alloys Compd 2019;790:837–46. https://doi.org/10.1016/j.jallcom.2019.03.162.

[16] Beyramali Kivy M., Asle Zaeem M., Lekakh S. Investigating phase formations in cast AlFeCoNiCu high entropy alloys by combination of computational modeling and experiments. Mater Des 2017;127:224–32. https://doi.org/10.1016/j.matdes.2017.04.086.

[17] Guo S., Ng C., Lu J., Liu C. T. Effect of valence electron concentration on stability of fcc or bcc phase in high entropy alloys. J Appl Phys 2011;109:103505. https://doi.org/10.1063/1.3587228.

[18] Priputen P., Noga P., Novaković M., Potočnik J., Antušek A., Bujdák R., et al. Unconventional order/disorder behaviour in Al–Co–Cu–Fe–Ni multi-principal element alloys after casting and annealing. Intermetallics 2023;162:108016. https://doi.org/10.1016/j.intermet.2023.108016.